Biocatalysis and Biotransformation

ISSN: 1024-2422 (Print) 1029-2446 (Online) Journal homepage: http://www.tandfonline.com/loi/ibab20

Production of (R)-3-quinuclidinol by a whole-cell biocatalyst with high efficiency

Zhenhua Jia, Hong Ma, Yali Huang, Yuanyuan Huang, Pengju Ren, Shuishan Song, Meirong Hu & Yong Tao

To cite this article: Zhenhua Jia, Hong Ma, Yali Huang, Yuanyuan Huang, Pengju Ren, Shuishan Song, Meirong Hu & Yong Tao (2017): Production of (R)-3-quinuclidinol by a whole-cell biocatalyst with high efficiency, Biocatalysis and Biotransformation, DOI: 10.1080/10242422.2017.1400019

To link to this article: http://dx.doi.org/10.1080/10242422.2017.1400019

BIOCATALYSIS AND BIOTRANSFORMATION, 2017
https://doi.org/10.1080/10242422.2017.1400019

Taylor & Francis
Taylor & Francis Group

RESEARCH ARTICLE

Production of (*R*)-3-quinuclidinol by a whole-cell biocatalyst with high efficiency

Zhenhua Jia[a]*, Hong Ma[a]*, Yali Huang[a], Yuanyuan Huang[a], Pengju Ren[a], Shuishan Song[a], Meirong Hu[b] and Yong Tao[b]

[a]Biology Institute, Hebei Academy of sciences, Shijiazhuang, P. R. China; [b]CAS Key Laboratory of Microbial Physiological and Metabolic Engineering, Institute of Microbiology, Chinese Academy of Sciences, Beijing, P.R. China

ABSTRACT

Optically pure (*R*)-3-quinuclidinol [(*R*)-3-Qui] is widely used as a chiral building block for producing various antimuscarinic agents. An asymmetric bioreduction approach using 3-quinuclidinone reductases is an effective way to produce (*R*)-3-Qui. In this study, a biocatalyst for producing (*R*)-3-Qui was developed by using *Escherichia coli* that coexpressed *Kaistia granuli* (*Kg*QR) and mutant glucose dehydrogenase (GDH). *Kg*QR catalyses the synthesis of (*R*)-3-Qui through the efficient reduction of 3-quinuclidinone. The specific activity of recombinant *Kg*QR was 254 U/mg, and the Michaelis–Menten constant (K_m) for 3-quinuclidinone was 0.51 mM. The thermal stability of *Kg*QR was relatively high compared with *ArQR*. Approximately 73% of the residual activity remained after incubation in 0.2 M potassium phosphate buffer (KPB) (pH 7.0) for 8 h at 30 °C. In addition, 80% residual activity remained for the double-mutant GDH (Q252L and E170K) after incubation in a buffer (pH 7.0) for 8 h at 30 and 40 °C. 3-Quinuclidinone (242 g/L) can be reduced to (*R*)-3-Qui in 3 h by coexpressing *Kg*QR and mutant GDH in *E. coli*. The conversion rate reached 80.6 g/L/h, which is the highest reported to date. The results demonstrates that this whole-cell biocatalyst will have a great potential in industrial manufacturing.

ARTICLE HISTORY
Received 21 April 2017
Revised 7 October 2017
Accepted 26 October 2017

KEYWORDS
Whole-cell biocatalyst; (*R*)-3-quinuclidinol; 3-quinuclidinone reductase; *Kaistia granuli*; glucose dehydrogenase; 3-quinuclidinone

1. Introduction

Chiral compounds are essential building blocks of drugs with a market share of nearly 50% (Hoelsch et al. 2013; Karsten et al. 2015; Weyler and Heinzle 2015; Willrodt et al. 2017). Optically, pure Qui is an important chiral pharmaceutical intermediate. Different isomers of Qui [(*R*)-3-Qui or (*S*)-3-Qui] are widely used in different fields (Zhang et al. 2016). Optically pure (*R*)-3-Qui is widely used as a chiral building block for producing various antimuscarinic agents such as talsaclidine, solifenacin, aclidinium bromide, and revatropate (Leusch et al. 2000; Ishihara et al. 2004; Prat et al. 2009). For the production of (*R*)-3-Qui, chemical synthesis, enzymatic resolution, and asymmetric bioreduction have been developed. Chemical synthesis is one of the most efficient routes to produce (*R*)-3-quinculidinol. A previous study demonstrated that the chiral metal catalyst RuBr2 [(S,S)-xylskewphos] has been used to synthesize (*R*)-3-Qui with 88–90% enantiomeric excess (ee); however, the trace metal contamination left in the product and the high cost of chiral metal catalysts are unresolved difficulties in the pharmaceutical industry (Tsutsumi et al. 2009). Kinetic resolution of a racemic mixture of *n*-butyl-3-Qui with protease has also been used to produce (*R*)-3-Qui (Tsutsumi et al. 2009). After 24 h of reaction, (*R*)-3-Qui is accessed with an overall yield of 42% and an optical purity of 96% ee (Ikunaka 2004). However, the theoretical yield of the product is only 50%, when using the racemic substrate, which limits the industrial application. In recent years, more studies have been focusing on asymmetric bioreduction as a method to produce (*R*)-3-Qui because asymmetric reductions can generate highly optically pure products at a relatively low cost, and the process is environmentally friendly.

An asymmetric bioreduction approach was used to produce (*R*)-3-Qui using 3-quinuclidinone reductases. For catalysing the synthesis of (*R*)-3-Qui, 3-quinuclidinone reductase uses the substrate 3-quinuclidinone and requires cofactor NAD(P)H. To accelerate the bioreduction process, it is necessary to regenerate NAD(P)H from $NAD(P)^+$. There have been many reports on the regeneration of NAD(P)H via coupling reactions

CONTACT Meirong Hu hmr1211@126.com CAS Key Laboratory of Microbial Physiological and Metabolic Engineering, Institute of Microbiology, Chinese Academy of Sciences, Beijing, P.R. China
*These authors contributed equally to this work.

Supplemental data for this article can be accessed here.

using alcohol dehydrogenase (ADH) (Machielsen et al. 2009; Soni et al. 2015; van Rossum et al. 2016; Solanki et al. 2017), glucose/glucose dehydrogenase (GDH) (Nagao et al. 1992; Ramadas et al. 2013; Takeshita et al. 2014) and formate/formate dehydrogenase (Hoelsch et al. 2013). Many researchers have cloned GDH for the bioreduction reaction to regenerate NAD(P)H (Nagao et al. 1992; Kataoka et al. 1998; Schewe et al. 2008; Pham et al. 2013). However, the stability of these GDHs has been poor, and many studies have focused on increasing their thermal stability (Makino et al. 1989; Baik et al. 2003; Pire et al. 2001, 2004; Ding et al. 2013; Liang et al. 2013). The crystal structure of GDH (GlcDH) from *Bacillus megaterium* IWG3 has been determined (Yamamoto et al. 2001). It is a tetrameric protein composed of four identical subunits. The tetramer could rapidly dissociate into inactive monomers under high temperatures and alkaline conditions. Therefore, the poor stability of GDH from *Bacillus* sp. is the bottleneck in its practical industrial applications. Previous studies have indicated that introducing Q252L and E170K mutation sites can increase the stability of GDH (Baik et al. 2005).

A number of enzymes have been reported as asymmetric reductases to produce (*R*)-3-Qui, including *Rr*QR from *Rhodotorula rubra*, QNR and BacC from *Microbacterium luteolum* JCM 9174, and *Ar*QR from *Agrobacterium radiobacter* ECU2556 (Uzura et al. 2009; Isotani et al. 2012; Isotani et al. 2013; Zhang et al. 2013). Among these, *Ar*QR is the most efficient enzyme. Its specific activity using 3-quinuclidinone as a substrate was 200 U/mg, and a high yield of (*R*)-3-Qui (up to 916 g/L/day) was obtained using *Ar*QR. However, the thermal stability of *Ar*QR is poor. Therefore, there is a need for 3-quinuclidinone reductases with both high thermal stability and high substrate-binding affinity. Hou et al. (2012, 2014) reported that 3-quinuclidinone reductase from *A. tumefaciens* (*At*QR) have high substrate-binding affinity and enantioselectivity. However, the synthesis of (*R*)-3-Qui using *At*QR has not been studied and fully evaluated. In the present study, 3-quinuclidinone reductase from *Kaistia granuli* (*Kg*QR), which possesses 95% sequence similarity with *At*QR (GenBank:3AK4_A), was expressed in *Escherichia coli*. According to above evidence, we hypothesized that *Kg*QR produces (*R*)-3-Qui from 3-quinuclidinone with high efficiency and enantioselectivity. In the present study, GDH from *B. megaterium* was cloned and used to regenerate NAD(P)H. Double-mutant Q252L and E170K GDH was constructed to produce (*R*)-3-Qui more efficiently. *Kg*QR was expressed, purified, and characterized. In addition, a whole-cell biocatalyst was constructed to produce (*R*)-3-Qui by coexpressing *Kg*QR and double-mutant GDH.

2. Material and methods

2.1. Strains, reagents, and enzymes

Escherichia coli DH5α was used for DNA manipulation. *Escherichia coli* K12/BW25113 (Keio collection, National BioResource Project NIG, Tokyo, Japan) was used for protein expression. *Bacillus megaterium* ATCC 14581 was obtained from ATCC. Vector pBAD–hisB (Invitrogen, Carlsbad, CA) was used for gene expression. 3-Quinuclidinone hydrochloride was obtained from Sigma-Aldrich Chemical Co. (Milwaukee, WI). (*R*)-3-Qui and (S) 3-Qui were purchased from Santa Cruz Biotechnology, Inc. (Santa Cruz, CA). Other commercial reagents were purchased in the highest purity available. All restriction enzymes, Pfu DNA polymerase, T4 DNA ligase, and Gibson Assembly™ Master Mix were obtained from New England Biolabs (Ipswich, UK).

2.2. Construction of expression plasmids

Standard methods were used for genomic DNA and plasmid DNA extraction, plasmid construction, and transformation (Sambrook and Russell 2001). Five plasmids, pBAD–hisB–*Kg*QR, pBAD–hisB–*Ar*QR, pBAD–hisB–*Bm*GDH, pBAD–hisB–*Q252LE170K*, and pBAD–hisB–QG, were constructed. pBAD–hisB–*Kg*QR was constructed as follows: the gene encoding *Kg*QR was synthesized on the basis of the protein sequence of 3-ketoacyl-ACP reductase (GenBank: WP_029076252) in GenScript USA Inc. (Township, NJ). The nucleotide sequence of *Kg*QR has been deposited in the GenBank databases (GenBank: AB733448). The gene fragment encoding *Kg*QR with restriction enzymes XhoI and PstI was inserted into pBAD–hisB at the same enzyme sites to generate pBAD–hisB–*Kg*QR. pBAD/hisB–*Ar*QR was constructed as follows: the gene encoding *Ar*QR (GenBank: YP_002542435.1), which was synthesized in GenScript USA Inc., was inserted into pBAD–hisB at the sites of restriction enzymes XhoI and PstI to form pBAD–hisB–*Ar*QR. pBAD–hisB–*Bm*GDH was constructed as follows: the gene encoding *Bm*GDH (GenBank: CP009920.1) was amplified by PCR using primers P1 and P2 with genomic DNA of *B. megaterium* ATCC 14581 as the template and inserted into pBAD–hisB at the sites of XhoI and PstI to generate pBAD–hisB–*Bm*GDH. To construct pBAD–hisB–*Q252LE170K*, PCR was performed using the primers shown in Supplementary Table S1 (P3 and P4, and P5 and P6 in succession) with pBAD–hisB–*Bm*GDH as

a template. The PCR products were digested with DpnI and transformed in *E. coli* DH5α to generate mutants. To construct pBAD–hisB–QG, which was used to reduce 3-quinuclidinone to (*R*)-3-Qui, the gene fragment encoding Q252LE170K was amplified by PCR using the primers P7 and P8 with pBAD–hisB–Q252LE170K encoding Q252LE170K was amplified by PCR using P7 and P8 with Pbad–hisBq as a template and then assembled with pBAD–hisB–*Kg*QR digested with PstI using Gibson Assembly™ Master Mix to generate pBAD–hisB–QG. After DNA sequencing, the appropriate plasmids were used to transform *E. coli* K12/BW25113 to express recombinant enzymes or as a whole-cell biocatalyst to produce (*R*)-3-Qui.

2.3. Cloning, expression, and purification

Recombinant BW25113 cells harboring expression vectors were cultured in 200 mL of 2YT broth (1.6% tryptone, 1.0% yeast extract, 0.5% NaCl) containing 100 μg/mL ampicillin. Following this, 0.2% arabinose was added until the OD_{600} reached 0.6, and the solution was incubated at 25 °C for further 13 h. The cells were then harvested by centrifugation (7000*g* for 10 min at 4 °C). The expressed *Kg*QR, *Ar*QR, *Bm*GDH, and Q252LE170K with N-terminal 6× His-tag were purified using an immobilized nickel-ion chromatography using an ÄKTA FPLC system GE Healthcare (Piscataway, NJ) equipped with a HisTrap HP column, according to the manufacturer's instructions. The bound recombinant *Kg*QR, *Ar*QR, *Bm*GDH, and Q252LE170K were eluted with an elution buffer [50 mM NaH_2PO_4, 300 mM NaCl, and 250 mM imidazole (pH 7.0)], and the elution fraction containing the recombinant enzymes was dialysed with 20 mM sodium phosphate buffer (pH 7.4) to remove excess imidazole. The purified recombinant enzymes were confirmed using sodium dodecyl sulphate–polyacrylamide gel electrophoresis (SDS–PAGE) electrophoresis containing a 10% (w/v) acrylamide gel. Protein concentrations were determined using the method of Bradford (1976) with bovine serum albumin as a standard. Purified recombinant enzymes were used to perform enzyme characterization assays.

2.4. Enzyme activity and kinetic parameters assay

A spectrophotometric assay of 3-quinuclidinone reductase activity was performed by measuring the decrease in absorbance of NADH at 340 nm ($\varepsilon = 6.22\ mMcm^{-1}$). The reaction mixture consisted of 200 μM 3-quinuclidinone hydrochloride, 0.1 mM NADH, 0.2 M KPB (pH 7.0), and 10 μL enzyme solution in a total volume of 1.0 mL. One unit of enzyme activity was defined as the amount of enzyme that catalyses the oxidation of 1 μmol of NADH/min under these conditions. The activity of *Bm*GDH was calculated by measuring the increase in absorbance of NADH at 340 nm. The reaction mixture contained 2 mM NAD^+, 0.1 M glucose, 0.2 M KPB (pH 7.0), and an appropriate amount of enzyme in a total volume of 1 mL. One unit of enzyme activity was defined as the amount of enzyme that catalyses the generation of 1 μmol NADH/min under these conditions. K_m values were obtained by assaying 3-quinuclidinone reductase activity in a range of substrate concentrations from 0.1 to 5.0 mM for 3-quinuclidinone and from 0.01 to 0.25 mM for NADH. The resulting curves were fitted to the Michaelis–Menten equation by non-linear least squares regression using Sigma Plot 11.0 (Systat Software, Chicago, IL) (K_m). The activity for each concentration was assayed in triplicate, resulting in a mean value for each substrate concentration. Data are the mean value of three independent measurements.

2.5. Thermal stability of KgQR, ArQR, BmGDH, and the Q252LE170K mutant

The thermal stability of *Kg*QR, *Ar*QR, *Bm*GDH, and the Q252LE170K mutant was determined by incubating the purified recombinant enzymes at different temperatures (30 °C for *Kg*QR and *Ar*QR; 30 and 40 °C for *Bm*GDH and the Q252LE170K mutant GDH, respectively) in 0.2 M KPB (pH 7.0) for 8 h. Samples were collected at different time intervals, and the residual activity was assayed under standard conditions. Data are the mean value of three independent measurements with standard deviations.

2.6. Product analysis by GC

The enantiomeric purity of (*R*)-3-Qui was analysed using a GC system (HP 6890; Hewlett Packard, Palo Alto, CA) equipped with a chiral capillary column (CP-cyclodextrin-N-236-N19, 0.25 mm × 25 m; Varian Medical Systems, Palo Alto, CA) with a flame ionization detector. The GC conditions were as follows: the column temperature program was increased to 120 °C, maintained for 10 min, and then ramped from 120 to 150 °C at 0.5 °C/min. The injection and detection temperatures were 220 °C. The retention times were 14.28 min for 3-quinuclidinone, 32.17 min for (*S*)-3-Qui, and 33.249 min for (*R*)-3-Qui.

2.7. Conversion of 3-quinuclidinone to (R)-3-Qui using a whole-cell biocatalyst

To construct the highly efficient whole-cell biocatalyst, the plasmid pBAD–hisB–QG containing *Kg*QR and the Q252LE170K mutant was used to transform *E. coli* K12/BW25113 to generate *E. coli* K12/BW25113 (pBAD–hisB–QG). The 3-quinuclidinone conversion reaction was performed using the *E. coli* whole-cell biocatalyst. The reaction mixture consisted of 65 mL of 200 mM pH 7.0 KPB, 2 M 3-quinuclidinone hydrochloride (242 g/L), 2 M glucose (360 g/L), 0.1 mM NAD^+, and 0.65 g of lyophilized cells of *E. coli* K12/BW25113 (pBAD–hisB–QG). The reaction mixture was stirred at 30 °C with pH adjustment to 7.0 by the automatic addition of a 2 M NaOH solution. The reaction mixture was sampled at appropriate intervals, and the production of (*R*)-3-Qui was analysed. Samples were alkalified with NaOH and extracted twice with an equal volume of ethyl acetate. The collected organic phases were combined and analysed by GC.

3. Results

3.1. Sequence analysis of 3-quinuclidinone-reducing enzymes

3-Quinuclidinone reductase from *Kg*QR (GenBank: WP_029076252) was isolated on the basis of the assumption that this enzyme would possess 95% sequence similarity with *At*QR. Sequence analysis indicated that *Kg*QR belonged to the short-chain dehydrogenases/reductases (SDR) family. The enzyme consisted of 260 amino acid residues with a calculated molecular mass of 27437.55 Da. The sequence of 3-quinuclidinone reductase displayed moderate identities with the NADH-dependent 3-quinuclidinone reductase *Ar*QR (~67%) (GenBank: YP_002542435.1) (Figure 1(A)). It also showed a low identity with NADPH-dependent 3-quinuclidinone reductase from *R. rubra* (25.61%) (GenBank: BAH28833.1) (Figure 1(A)). The results indicated that *Kg*QR be probably NADH-dependent 3-quinuclidinone reductase with high specific activity.

3.2. Gene cloning, enzyme expression, and purification

The gene encoding *Kg*QR and *Ar*QR was synthesized on the basis of the codon usage of *E. coli*. It has been submitted to GenBank (The GenBank numbers of KgQR and ArQR were KT228249 and KT228250, respectively). *Bm*GDH (GenBank: CP009920.1) was amplified using the genome of *B. megaterium* ATCC 14581 as a template with the primers GDHF and GDHR (Supplementary Table S1). Three expression vectors, pBAD–*Kg*QR, pBAD–*Ar*QR, and pBAD–*Bm*GDH, which encoded *Kg*QR, *Ar*QR, and *Bm*GDH, respectively, were constructed. pBAD–hisB–Q252LE170K was constructed on the basis of pBAD–*Bm*GDH (see "Material and Methods" section for details). ORFs for these genes were fused with an N-terminal 6 × His-tag. Recombinant BW25113 cells harboring expression vectors were cultured at 37 °C until the OD_{600} was 0.6. Then, the expression of recombinant cells were induced by 0.2% arabinose. *Kg*QR, *Ar*QR, *Bm*GDH, and mutant GDH were purified by Ni–NTA agarose column chromatography. Homogeneous purification was confirmed by SDS–PAGE (Figure 1(B,C)). SDS–PAGE revealed that the molecular masses of recombinant *Ar*QR, *Kg*QR, and *Bm*GDH were 28, 25, and 37 kDa, respectively. SDS–PAGE of GDH mutant (not shown) was the same as that of *Bm*GDH. The four enzymes expressed in *E. coli* were soluble.

3.3. Characterization of recombinant KgQR, ArQR, BmGDH, and the Q252LE170K mutant

The K_m values of purified recombinant *Kg*QR and *Ar*QR for 3-quinuclidinone in the reductive reaction were 0.52 and 0.91 mM, respectively, from the Hanes–Woolf plot. The K_m value of purified KgQR for 3-quinuclidinone was lower than that of ArQR. It indicated that the reaction velocity will be high even with a low concentration of 3-quinuclidinone, as for *Kg*QR. The K_m values of *Kg*QR and *Ar*QR for NADH in the reductive reaction were 0.03 and 0.028 mM (Table 1), respectively. The specific activities of *Kg*QR and *Ar*QR were 254 and 200 U/mg, respectively. The specific activities of *Bm*GDH and the Q252LE170K mutant were 356.9 and 350.0 U/mg (Table 1), respectively. The effect of pH on recombinant *Kg*QR, *Ar*QR, *Bm*GDH, and the Q252LE170K mutant was measured using various pH buffers; our results indicated that the maximum activity of these enzymes was at pH 7.0.

3.4. Thermal stability of KgQR, ArQR, BmGDH, and the Q252LE170K mutant

The thermal stability of *Kg*QR, *Ar*QR, *Bm*GDH, and the Q252LE170K mutant was determined using purified recombinant enzymes (Figure 2(A,B)). The results indicated that the thermal stability of *Kg*QR was relatively high and a residual activity of ~73% remained after incubation in 0.2 M KPB (pH 7.0) for 8 h at 30 °C. In contrast, the residual activity of *Ar*QR was only about 25% (Figure 2(A)). The thermal stability of *Bm*GDH was

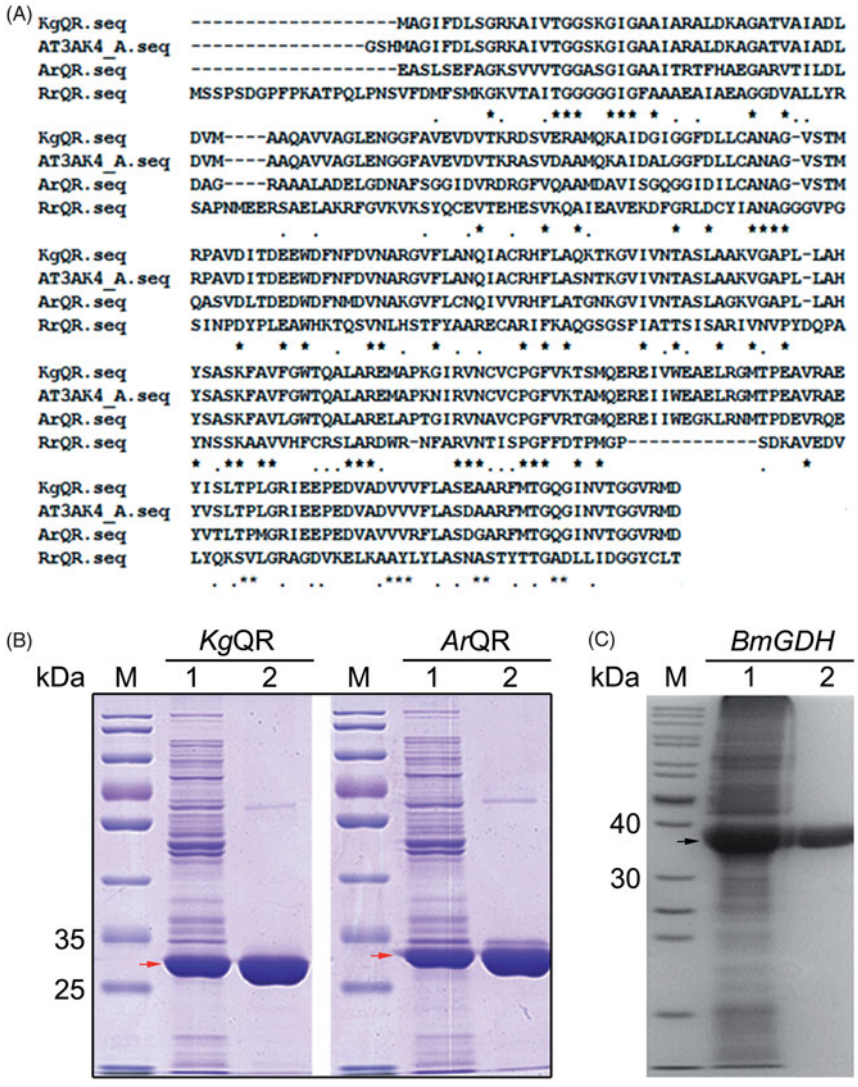

Figure 1. Comparison of amino acid sequences and SDS–PAGE analysis of purified 3-quinuclidinone reductases from different organisms *K. granuli* and those of SDR superfamily proteins. (A) *Kg*QR (GenBank: WP_018183582.1) from *Kaistia granuli*, AT3AK4 (GenBank: 3AK4_A) from *Agrobacterium tumefaciens*, *Ar*QR (GenBank: YP_002542435.1) from *A. radiobacter* ECU2556, and *Rr*QR (GenBank: BAH28833.1) from *R. rubra*. Multiple sequence alignment was performed using the DNAMAN program. (B) SDS–PAGE analysis of recombinant *Kg*QR, and *Ar*QR. M: Mark; 1: *E. coli* K12/pBAD–*Kg*QR, *E. coli* K12/pBAD–*Ar*QR; 2: the purified recombinant enzymes *Kg*QR, *Ar*QR. (C) SDS–PAGE analysis of recombinant *Bm*GDH. M: Mark; 1: *E. coli* K12/pBAD–*Bm*GDH; 2: the purified recombinant enzyme *Bm*GDH.

Table 1. Characterization of recombinant *Kg*QR, *Ar*QR, *Bm*GDH, and the Q252LE170K mutant.

Property	NADH K_m (mM)	3-Quinuclidinone K_m (mM)	Specific activity (U/mg)	Stereoselectivity for (*R*)-3-quinuclidinol (%)	Optimum pH
*Kg*QR	0.030	0.52	251.41	>99.9	7–7.5
*Ar*QR	0.028	0.91	200.23	>99.9	7
*Bm*GDH			356.95		7
Q252LE170K mutant			350.00		7

very low, and 10% residual activity remained after incubation in buffer (pH 7.0) for 1.5 h at 30 °C. The Q252LE170K mutant showed good thermal stability, and 80% residual activity after incubation in buffer (pH 7.0) for 8 h at both 30 and 40 °C (Figure 2(B)).

3.5. Production of (R)-3-Qui using a whole-cell biocatalyst containing KgQR and the Q252LE170K mutant in E. coli cells

Highly efficient production of (*R*)-3-Qui was obtained using coexpressed 3-quinuclidinone reductase and

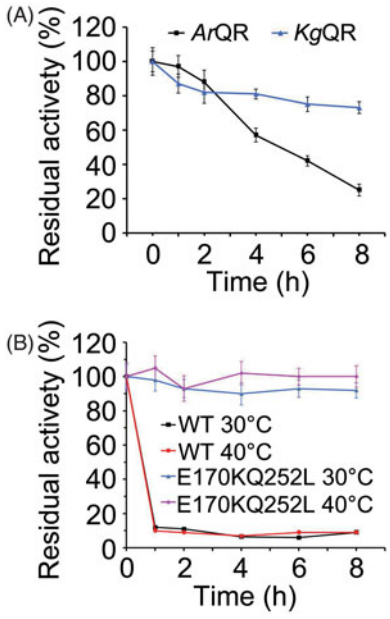

Figure 2. Thermostability of 3-quinuclidinone reductases. (A) Thermostability of *Ar*QR and *Kg*QR. (B) Thermostability of WT (*Bm*GDH) and Q252LE170K at 30 and 40 °C, respectively.

GDH with good catalytic properties. Our results indicated that the specific activity of *Kg*QR was higher than that of *Ar*QR and the thermal stability of *Kg*QR was considerably better than that of *Ar*QR. The thermal stability of the Q252LE170K mutant was considerably better than that of WT. Therefore, *Kg*QR and the Q252LE170K mutant were used to construct a whole-cell biocatalyst by transforming pBAD–hisB–QG into *E. coli* K12/BW25113. According to previous studies (Tomoko et al. 2000; Hou et al. 2014), the conversion rate can be increased by adding NAD^+. Therefore, 0.1 mM NAD^+ was added to the reaction mixture, and 242 g/L of the substrate was loaded. After 3 h of the reaction, the substrate was completely converted to (*R*)-3-Qui (Figure 3). The conversion rate in the present study was 80.6 g/L/h. GC analysis of the product indicated that the optical purity of the (*R*)-3-Qui produced by *Kg*QR was 99% ee, which was same as that produced by *Ar*QR (Table 1).

4. Discussion

(*R*)-3-Qui is a useful compound applicable to the synthesis of various pharmaceuticals (Rzeszotarski et al. 1988; Ishihara et al. 2004). Using carbonyl reductases catalysing the asymmetric reduction of 3-quinuclidinone to (*R*)-3-Qui have been attempted, such as reductases of *Datura stramonium* (Portseffen et al. 1994) and *Hyoscyamus niger* (Hashimoto et al. 1992), *Rr*QR of *R. rubra* (Uzura et al. 2009), QNR and BacC from *M. luteolum* JCM 9174 (Isotani et al. 2012), and *Ar*QR

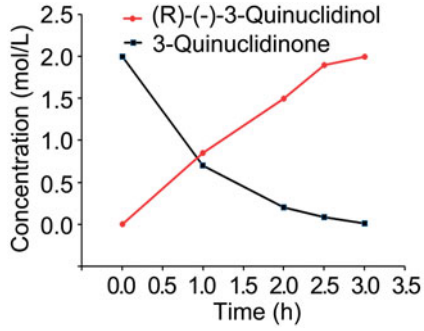

Figure 3. Time course of production of (*R*)-3-Qui by *E. coli* biocatalyst containing pBAD–hisB–QG. The concentration of (*R*)-3-Qui is represented by a solid circle and that of 3-quinuclidinone by a solid square. Data are the mean value of three independent measurements with standard deviation.

from *A. radiobacter* ECU2556 (Zhang et al. 2013). In the present study, a novel and efficient whole-cell biocatalyst was constructed to produce (*R*)-3-Qui. Using *E. coli* K12/BW25113 (pBAD–hisB–QG) coexpressing the 3-quinuclidinone reductase and double-mutant GDH, 27thinsp;M (242 g/L) 3-quinuclidinone hydrochloride was stereospecifically converted to (*R*)-3-Qui with 99% conversion in 3 h (Figure 3). The conversion rate reached 80.6 g/L/h, which is higher than that reported by Zhang et al. (2013). In that study, 2 M (242 g/L) 3-quinuclidinone hydrochloride was completely converted to (*R*)-3-Qui with 99% conversion and >99% ee within 4.5 h, and the conversion rate was only 53.7 g/L/h.

The efficient biocatalyst system in the present study was based on a 3-quinuclidinone reductase with good catalytic features and GDH with high specific activity and thermal stability. *Kg*QR can be widely used for the production of (*R*)-3-Qui because of its catalytic feature. The K_m value (0.51 mM) of *Kg*QR for 3-quinuclidinone in the reductive reaction was much lower than that of *Rr*QR (145 mM) (Uzura et al. 2009) and even lower than that of *Ar*QR (0.91 mM) (Table 1). The specific activity of *Kg*QR (254 U/mg) was higher than that of *Ar*QR (200 U/mg). Furthermore, the thermal stability of *Kg*QR was better than that of *Ar*QR. The activity of *Kg*QR was relatively high, and up to 75% residual activity remained after incubation in 0.2 M KPB buffer (pH 7.0) for 8 h at 30 °C. These results also imply that the conformation of KgQR is more favourable to the catalytic reaction than that of ArQR. *Kg*QR is an NADH-dependent 3-quinuclidinone reductase. For the large-scale production of (*R*)-3-Qui, NAD^+, which is less expensive than $NADP^+$, can be added to the reaction buffer. Therefore, NADH-dependent quinuclidinone reductase is more suitable for the production of (*R*)-3-Qui. The Q252LE170K mutant also had good

thermal stability. It was incubated in a buffer (pH 7.0) for 8 h at 30 and 40 °C, with 80% residual activity remaining. Therefore, in our study, a highly efficient whole-cell biocatalyst system was obtained using *Kg*QR with good catalytic properties and a Q252LE170K mutant with high stability. A high yield of (*R*)-3-Qui, greater than 200 g/L, was obtained in 3 h. The conversion rate based on substrate was 80.6 g/L/h, demonstrating that the process has a great potential for the industrial production.

In the present study, we developed a highly efficient whole-cell biocatalyst to produce (*R*)-3-Qui by coexpressing *Kg*QR and the Q252LE170K mutant (GDH) in *E. coli*. Our result indicated that *Kg*QR has good catalytic features such as high specific activity, substrate affinity, stereoselectivity, and thermal stability. The thermal stability of GDH was clearly increased by introducing *Q252L* and *E170K* mutations. The maximum conversion rate of 80.6 g/L/h, which was achieved by the whole-cell biocatalyst coexpressing *Kg*QR and the Q252L and E170K mutant GDH, demonstrates that this whole-cell biocatalyst has a great effect on industrial manufacturing.

Disclosure statement

The authors declare that they have no potential conflict of interests.

Funding

This study was supported by the Science Foundation of Hebei Science Academy [Grant Nos. 12342, 15004022 and 2016023290-01] and Hebei High Technology Plan [Grant No. 16212801D].

References

Baik SH, Ide T, Yoshida H, Kagami O, Harayama S. 2003. Significantly enhanced stability of glucose dehydrogenase by directed evolution. Appl Microbiol Biotechnol 61:329–335.

Baik SH, Michel F, Aghajari N, Haser R, Harayama S. 2005. Cooperative effect of two surface amino acid mutations (Q252L and E170K) in glucose dehydrogenase from *Bacillus megaterium* IWG3 on stabilization of its oligomeric state. Appl Environ Microbiol 71:3285–3293.

Bradford MM. 1976. A rapid and sensitive method for the quantitation of microgram quantities of protein utilizing the principle of protein-dye binding. Anal Biochem 72:248–254.

Ding H, Gao F, Liu D, Li Z, Xu X, Wu M, Zhao Y. 2013. Significant improvement of thermal stability of glucose 1-dehydrogenase by introducing disulfide bonds at the tetramer interface. Enzyme Microb Technol 53:365–372.

Hashimoto T, Nakajima K, Ongena G, Yamada Y. 1992. Two tropinone reductases with distinct stereospecificities from cultured roots of *Hyoscyamus niger*. Plant Physiol 100: 836–845.

Hoelsch K, Suhrer I, Heusel M, Weuster-Botz D. 2013. Engineering of formate dehydrogenase: synergistic effect of mutations affecting cofactor specificity and chemical stability. Appl Microbiol Biotechnol 97:2473–2481.

Hou F, Miyakawa T, Kataoka M, Takeshita D, Kumashiro S, Uzura A, Urano N, Nagata K, Shimizu S, Tanokura M. 2014. Structural basis for high substrate-binding affinity and enantioselectivity of 3-quinuclidinone reductase AtQR. Biochem Biophys Res Commun 446:911–915.

Hou F, Miyakawa T, Takeshita D, Kataoka M, Uzura A, Nagata K, Shimizu S, Tanokura M. 2012. Expression, purification, crystallization and X-ray analysis of 3-quinuclidinone reductase from Agrobacterium tumefaciens. Acta Crystallogr F Struct Biol Cryst Commun 68:1237–1239.

Ikunaka M. 2004. Biocatalysis from the perspective of an industrial practitioner: let a biocatalyst do a job that no chemocatalyst can. Catalysis Today 96:93–102.

Ishihara T, Kakuta H, Moritani H, Ugawa T, Yanagisawa I. 2004. Synthesis and biological evaluation of quinuclidine derivatives incorporating phenothiazine moieties as squalene synthase inhibitors. Chem Pharm Bull 52:1204–1209.

Isotani K, Kurokawa J, Itoh N. 2012. Production of (R)-3-quinuclidinol by *E. coli* biocatalysts possessing NADH-dependent 3-quinuclidinone reductase (QNR or bacC) from *Microbacterium luteolum* and Leifsonia alcohol dehydrogenase (LSADH). Int J Mol Sci 13:13542–13553.

Isotani K, Kurokawa J, Suzuki F, Nomoto S, Negishi T, Matsuda M, Itoh N. 2013. Gene cloning and characterization of two NADH-dependent 3-quinuclidinone reductases from *Microbacterium luteolum* JCM 9174. Appl Environ Microbiol 79:1378–1384.

Karsten L, Katja B, Andreas S. 2015. Multistep synthesis of (S)-3-hydroxyisobutyric acid from glucose using *Pseudomonas taiwanensis* VLB120 B83 T7 catalytic biofilms. Adv Synth Catal 357:1919–1927.

Kataoka M, Sri Rohani LP, Wada M, Kita K, Yanase H, Urabe I, Shimizu S. 1998. *Escherichia coli* transformant expressing the glucose dehydrogenase gene from *Bacillus megaterium* as a cofactor regenerator in a chiral alcohol production system. Biosci Biotechnol Biochem 62:167–169.

Leusch A, Troger W, Greischel A, Roth W. 2000. Pharmacokinetics of the M1-agonist talsaclidine in mouse, rat, rabbit and monkey, and extrapolation to man. Xenobiotica 30:797–813.

Liang B, Lang Q, Tang X, Liu A. 2013. Simultaneously improving stability and specificity of cell surface displayed glucose dehydrogenase mutants to construct whole-cell biocatalyst for glucose biosensor application. Bioresour Technol 147:492–498.

Machielsen R, Looger LL, Raedts J. 2009. Cofactor engineering of *Lactobacillus brevis* alcohol dehydrogenase by computational design. Eng Life Sci 9:38–44.

Makino Y, Negoro S, Urabe I, Okada H. 1989. Stability-increasing mutants of glucose dehydrogenase from *Bacillus megaterium* IWG3. J Biol Chem 264:6381–6385.

Nagao T, Mitamura T, Wang XH, Negoro S, Yomo T, Urabe I, Okada H. 1992. Cloning, nucleotide sequences, and enzymatic properties of glucose dehydrogenase

isozymes from *Bacillus megaterium* IAM1030. J Bacteriol 174:5013–5020.

Pham SQ, Gao P, Li Z. 2013. Engineering of recombinant *E. coli* cells co-expressing P450pyrTM monooxygenase and glucose dehydrogenase for highly regio- and stereoselective hydroxylation of alicycles with cofactor recycling. Biotechnol Bioeng 110:363–373.

Pire C, Esclapez J, Ferrer J, Bonete MJ. 2001. Heterologous overexpression of glucose dehydrogenase from the halophilicarchaeonHaloferaxmediterranei, an enzyme of the medium chain dehydrogenase/reductase family. FEMS Microbiol Lett 200:221–227.

Pire C, Marhuenda-Egea FC, Esclapez J. 2004. Stability and enzymatic studies of glucose dehydrogenase from the Archaeon *Haloferax mediterranei* in reverse micelles. Biocatal Biotransform 22:17–23.

Portseffen A, Dräger B, Nahrstedt A. 1994. The reduction of tropinone in *Datura stramonium* root cultures by two specific reductases. Phytochemistry 37:391–400.

Prat M, Fernandez D, Buil MA, Crespo MI, Casals G, Ferrer M, Tort L, Castro J, Monleon JM, Gavalda A, et al. 2009. Discovery of novel quaternary ammonium derivatives of (3R)-quinuclidinol esters as potent and long-acting muscarinic antagonists with potential for minimal systemic exposure after inhaled administration: identification of (3R)-3-{[hydroxy(di-2-thienyl)acetyl]oxy}-1-(3-phenoxypropyl)-1-azoniabicyclo [2.2.2]octane bromide (aclidinium bromide). J Med Chem 52:5076–5092.

Ramadas C, Narayana RM, Srinivasa RC. 2013. Industrially viable preparation of *(R)-3-quinuclidinol*, a key building block of muscarine M1, M3 agonists and M3 antagonists. Org Prep Proc Int 45:507–509.

Rzeszotarski WJ, McPherson DW, Ferkany JW, Kinnier WJ, Noronha-Blob L, Kirkien-Rzeszotarski A. 1988. Affinity and selectivity of the optical isomers of 3-quinuclidinyl benzilate and related muscarinic antagonists. J Med Chem 31:1463–1466.

Sambrook J, Russell DW. 2001. Molecular cloning: a laboratory manual. Cold Spring Harbor: Laboratory Press.

Schewe H, Kaup BA, Schrader J. 2008. Improvement of P450 (BM-3) whole-cell biocatalysis by integrating heterologous cofactor regeneration combining glucose facilitator and dehydrogenase in *E. coli*. Appl Microbiol Biotechnol 78:55–65.

Solanki K, Abdallah W, Banta S. 2017. Engineering the cofactor specificity of an alcohol dehydrogenase via single mutations or insertions distal to the 2′-phosphate group of NADP(H). Protein Eng Des Sel 8:1–8.

Soni JY, Premasagar V, Thakore S. 2015. An improved and simple route for the synthesis of 3-quinuclidinone hydrochloride. Lett Org Chem 12:277–279.

Takeshita D, Kataoka M, Miyakawa T, Miyazono K, Kumashiro S, Nagai T, Urano N, Uzura A, Nagata K, Shimizu S, et al. 2014. Structural basis of stereospecific reduction by quinuclidinone reductase. AMB Express 4:1–6.

Tomoko M, Tadao H, Nobuyoshi N, Kaoru N. 2000. Mechanism for improving stereoselectivity for asymmetric reduction using acetone powder of microorganism. Tetreh 41:4135–4138.

Tsutsumi K, Katayama T, Utsumi N. 2009. Practical asymmetric hydrogenation of 3-quinuclidinone catalyzed by the XylSkewphos/PICA-Ruthenium(II) complex. Org Process Res Dev 13:625–628.

Uzura A, Nomoto F, Sakoda A, Nishimoto Y, Kataoka M, Shimizu S. 2009. Stereoselective synthesis of (R)-3-quinuclidinol through asymmetric reduction of 3-quinuclidinone with 3-quinuclidinone reductase of *Rhodotorula rubra*. Appl Microbiol Biotechnol 83:617–626.

Van Rossum HM, Kozak BU, Pronk JT, van Maris AJ. 2016. Engineering cytosolic acetyl-coenzyme A supply in *Saccharomyces cerevisiae*: pathway stoichiometry, free-energy conservation and redox-cofactor balancing. Metab Eng 36:99–115.

Weyler C, Heinzle E. 2015. Multistep synthesis of UDP-glucose using tailored, permeabilized cells of *E. coli*. Appl Biochem Biotechnol 175:3729–3736.

Willrodt C, Halan B, Karthaus L, Rehdorf J, Julsing MK, Buehler K, Schmid A. 2017. Continuous multistep synthesis of perillic acid from limonene by catalytic biofilms under segmented flow. Biotechnol Bioeng 114:281–290.

Yamamoto K, Kurisu G, Kusunoki M, Tabata S, Urabe I, Osaki S. 2001. Crystal structure of glucose dehydrogenase from *Bacillus megaterium* IWG3 at 1.7 A resolution. J Biochem 129:303–312.

Zhang Y, Feng J, Li J, Wang Y, Wang M. 2016. Asymmetric enzymatic reduction of quinuclidinone to (S)-3-quinuclidinol. Chin J Appl Environ Biol 22:0854–0859.

Zhang WX, Xu GC, Huang L, Pan J, Yu HL, Xu JH. 2013. Highly efficient synthesis of (R)-3-quinuclidinol in a space-time yield of 916 g L(-1) d(-1) using a new bacterial reductase ArQR. Org Lett 15:4917–4919.